

# Preparation, structural and electrical characteristics of praseodymium modified lead titanate

Vishal Singh, K.K. Bamzai<sup>\*</sup>, Shivani Suri, Nidhi

*Crystal Growth & Materials Research Laboratory, Department of Physics and Electronics, University of Jammu, Jammu 180006, India*

Received 10 January 2011; received in revised form 6 April 2011; accepted 7 April 2011

Available online 14 April 2011

## Abstract

Praseodymium modified lead titanate ceramics ( $\text{Pb}_{1-x}\text{Pr}_x\text{Ti}_{1-2y}\text{Mo}_y\text{Fe}_y\text{O}_3$ ) with  $x = 0.02, 0.04, 0.06, 0.08$  and  $0.10$  and  $y = 0.02$  have been prepared by high temperature solid state reaction technique. Cold pressed pellets were sintered at  $1100^\circ\text{C}$  for 2 h. Lattice parameters and crystal tetragonality was determined by X-ray diffraction analysis. All the synthesized samples show single phase with tetragonal structure. Tetragonality decreases and relative density increases with the increase in praseodymium substitution. Electrical characteristics which include dielectric properties and ac conductivity were studied as a function of temperature and frequency. Variation of dielectric constant with temperature shows a ferroelectric phase transition and transition temperature ( $T_C$ ) decreases with increase in the praseodymium content. Nature of transition was studied and found to be diffused. Conductivity ( $\sigma_{ac}$ ) was measured as a function of frequency in the range  $10^3$ – $10^6$  Hz at different temperature suggesting hopping mechanism.

© 2011 Elsevier Ltd and Techna Group S.r.l. All rights reserved.

**Keywords:** B. Grain size; C. Dielectric properties; C. Electrical conductivity; Solid state reaction

## 1. Introduction

Ferroelectric materials based on the perovskite structure are of great interest in microelectronics, finding applications in pyroelectric and piezo-electric devices, actuators, sensors, non-volatile memories and optical wave guides [1].  $\text{ABO}_3$  type of perovskite compounds, such as  $\text{BaTiO}_3$ ,  $\text{SrTiO}_3$  and  $\text{PbTiO}_3$  have drawn a great deal of attention due to their ferroelectric and electro-optic properties [2–4].

Among the many ferroelectric oxides with perovskite structure, some of them are in the forefront both in the area of research as well as in industrial applications. Lead titanate (PT) is one of the most highly investigated ferroelectric materials both in thin film and bulk forms owing to its superior ferroelectric properties [5]. However, this material has poor mechanical properties due to its large tetragonal strain which makes poling of PT material difficult. Also, it is very difficult to produce pure and dense PT because of its porous and fragile

nature due to high vapour and tetragonal distortion. Hence, much attention has been focused on the modification of PT by doping with the purpose of obtaining improved mechanical and electrical properties. The incorporation of off-valent ( $\text{La}^{3+}$ ,  $\text{Sm}^{3+}$ ,  $\text{Gd}^{3+}$ , etc.) and isovalent ( $\text{Ca}^{2+}$ ,  $\text{Ba}^{2+}$ ,  $\text{Sr}^{2+}$ ) ions into  $\text{Pb}^{2+}$  site is reported to enhance the mechanical stability along with good dielectric, ferroelectric and piezoelectric properties [6]. The substitution of these ions results in the reduction of lattice anisotropy leading to hard and dense ceramic with high mechanical strength [7–9]. Doping reduces Curie temperature of PT ceramics, which for pure PT ceramics is high ( $490^\circ\text{C}$ ). Dielectric and piezoelectric properties of Sm modified PT ceramic prepared by solid state reaction method has been studied by Tickoo et al. [10]. In the present investigations, experiments were performed aiming at substitution of  $\text{Pr}^{3+}$  ion into  $\text{Pb}^{2+}$  sites whereas Fe and Mo in Ti sites partially. Modification of Fe is reported to produce ceramic of high mechanical quality factor [11]. Substitution of  $\text{Mo}^{6+}$  ions in  $\text{Ti}^{4+}$  site enhances the resistivity by compensation of charge due to off – valency substitution of  $\text{Pr}^{3+}$  in  $\text{Pb}^{2+}$  site. As a result, these modified (PT) ceramics will have high resistivity and high mechanical strength and can be subjected to severe poling conditions [7].

<sup>\*</sup> Corresponding author. Tel.: +91 191 2450939.

E-mail addresses: [kkbamz@yahoo.com](mailto:kkbamz@yahoo.com), [krishbamz@rediffmail.com](mailto:krishbamz@rediffmail.com) (K.K. Bamzai).

## 2. Experimental

The samples having composition  $\text{Pb}_{1-x}\text{Pr}_x\text{Ti}_{1-2y}\text{Mo}_y\text{Fe}_y\text{O}_3$  with  $x = 0.02, 0.04, 0.06, 0.08$  and  $0.10$  and  $y = 0.02$  were prepared by solid state reaction technique. Proportionate amount as per mole formula of starting material ( $\text{PbO}$ ,  $\text{TiO}_2$ ,  $\text{Pr}_6\text{O}_{11}$ ,  $\text{MoO}_3$ ,  $\text{Fe}_2\text{O}_3$ ) were weighed and wet mixed by milling for 48 h using zirconia balls as grinding media and distilled water as wetting agent. The slurry was dried in an oven. The dried powder was calcinated at  $800^\circ\text{C}$  for 2 h in the furnace. Calcinated powder was then compacted to form pellet of size 10 mm in diameter and 1–2 mm in thickness. Small amount of PVA was added which act as binder. All the samples were then sintered at a temperature of  $1100^\circ\text{C}$  for 2 h at a constant rate of heating ( $4^\circ\text{C}/\text{min}$ ). X-ray diffraction analysis was carried out at room temperature using x-ray diffractometer (Rigaku Co. Ltd. Japan) with  $\text{Cu K}\alpha$  radiation having wavelength ( $\lambda = 1.5405 \text{ \AA}$ ) in the range of Bragg angle  $2\theta$  ( $20^\circ \leq 2\theta \leq 70^\circ$ ) with scanning speed of  $2^\circ/\text{min}$ .

Microstructural study for Pr doped PT ceramics was done by using scanning electron microscope (LEO 435 VP). Gold coating was sprayed on the discs by using a turbo sputter coater for avoiding possible charging of specimen before SEM observation.

The dielectric properties were measured by using fully automated impedance analyzer 4192A-LF interfaced with USB-GPIB converter 82357 B (Agilent). For the measurements of dielectric constant and tangent loss as a function of temperature and frequency, the samples of thickness 1 mm and diameter 10 mm were polished with silver electrodes and then fired in an oven upto at  $400^\circ\text{C}$  for 1 h. The dielectric properties were then measured at different frequencies of 1, 5, 10, 20, 50, and 100 kHz in the temperature of range  $30\text{--}500^\circ\text{C}$ .

## 3. Results and discussions

### 3.1. Structural characteristics

Fig. 1 shows X-ray diffraction pattern of Pr modified ceramics with composition  $\text{Pb}_{1-x}\text{Pr}_x\text{Ti}_{1-2y}\text{Mo}_y\text{Fe}_y\text{O}_3$  with  $x = 0.02, 0.04, 0.06, 0.08, 0.10$  and  $y = 0.02$ . This diffraction

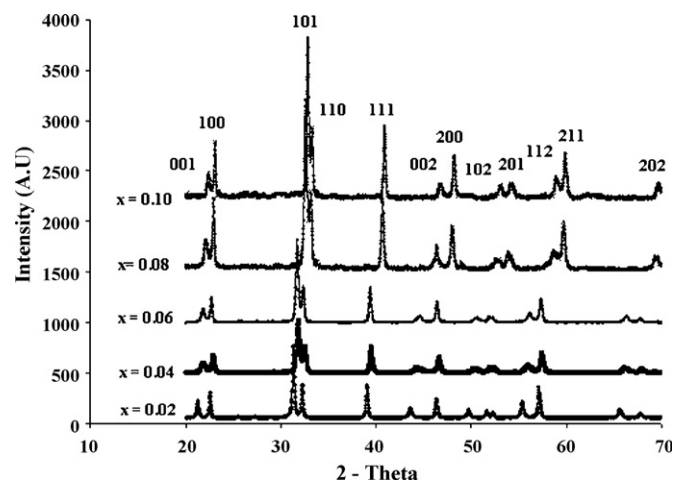


Fig. 1. X-ray diffraction pattern of  $\text{Pb}_{1-x}\text{Pr}_x\text{Ti}_{1-2y}\text{Mo}_y\text{Fe}_y\text{O}_3$  sintered at  $1100^\circ\text{C}$  for different compositions  $x = 0.02, 0.04, 0.06, 0.08, 0.10$  and  $y = 0.02$ .

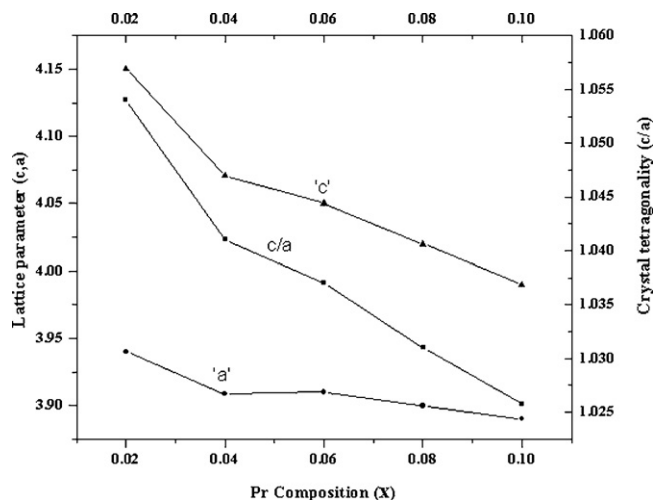


Fig. 2. Variation of lattice parameters ( $a$ ,  $c$ ) and lattice tetragonality ( $c/a$ ) with praseodymium substitution ( $x$ ).

pattern confirms single phase formation with tetragonal structure for all the composition. From the observed  $d$ -values, lattice parameters ( $a$  and  $c$ ) were computed and tetragonality ( $c/a$ ) was calculated and these are shown in Fig. 2. The value of ' $c$ ' decreases faster where as ' $a$ ' decreases first upto 0.04 and then remains almost constant. Crystal tetragonality ( $c/a$ ) is found to decrease with the increase in the Pr substitution content resulting in hard and dense ceramics [12]. This decrease in the tetragonality with the increase in Pr content clearly indicates that Pr ions enter the lattice on A-site replacing Pb ions. Therefore, it can be concluded that Pr substitution enhances the densification and stabilizes the sintered compositions to a high degree. The X-ray density of the prepared sample was calculated using the relation:  $\rho_{\text{X-ray}} = nM/a^2cN$ ; where ' $n$ ' is the number of molecules/unit cell  $\cong 1$ ,  $M$  is the molecular weight, ' $a$ ' and ' $c$ ' is the lattice parameter and ' $N$ ' is the Avogadro's number. The experimental density was calculated by considering the cylindrical shape and using the relation:  $\rho_{\text{ex}} = m/V = m/(\pi r^2 h)$ ; where ' $m$ ' is the mass, ' $r$ ' is the radius and ' $h$ ' is the thickness of the pellet. Porosity ' $P$ ' of the sample was calculated by employing relation:  $P = \rho_{\text{X-ray}} - \rho_{\text{ex}}/\rho_{\text{ex}} \times 100$ ; where ' $\rho_{\text{X-ray}}$ ' is theoretical density and ' $\rho_{\text{ex}}$ ' is experimental density in  $\text{gm}/\text{cm}^3$ .

The result of theoretical density, experimental density and porosity is given in tabular form (Table 1). It is found that experimental density increases from 92.94% to 94.62% of the theoretical density with the increase in praseodymium concentration from 2 to 10 mol%. The increase in experimental densities and reduction in porosity is due to the fact that increase in Pr content decreases the tetragonality in PT ceramic, because of its large spontaneous stress described as  $[T_s \propto (c/a - 1)]$  [7]. Reduction in internal stress allows the crystallites in grains to accommodate more closely to form a denser microstructure, which results in reduction in porosity and increase in density.

Fig. 3(a and b) shows scanning electron micrograph (SEM) of Pr modified PT ceramics with  $x = 0.04$  and  $0.10$ , respectively. It is found that well developed grains are observed in all compositions. SEM micrograph indicates that grains are nearly spherical and uniformly distributed throughout its

Table 1

Lattice constants ( $a$  &  $c$ ), tetragonality ( $c/a$ ), X-ray density, experimental density, porosity, relative density and grain size for different composition of Pr substituted in lead titanate.

$x$	$a$ (Å)	$c$ (Å)	$c/a$	$\rho_{\text{X-ray}}$ (g/cc)	$\rho_{\text{ex}}$ (g/cc)	Porosity	Relative density (in %)	Grain size (nm)
0.02	3.94	4.15	1.053	7.80	7.25	7.05	92.94	–
0.04	3.88	4.04	1.041	8.23	7.65	7.04	92.95	268
0.06	3.91	4.05	1.035	8.07	7.51	6.93	93.06	507
0.08	3.90	4.02	1.030	8.11	7.58	6.53	93.46	353
0.10	3.89	3.99	1.025	8.18	7.74	5.36	94.62	531

sample. The grain with no such voids confirms high density of the sample. Grain size has been measured by average line intercept (ALI) technique and is found to increase with the increase in Pr substitution except for 8 mole% where it shows decrease. The average grain size varies from 268 to 531 nm, the value of which is given in Table 1.

### 3.2. Electrical characteristics

#### 3.2.1. Dielectric properties

The temperature variation of dielectric constant ( $\epsilon'$ ) for different Pr composition at a frequency range  $10^3$ – $10^5$  Hz is shown in Fig. 4(a–d). As typical of normal ferroelectric,

dielectric constant ( $\epsilon'$ ) increases gradually with the temperature below the Curie temperature and then decreases with further increase in temperature. It can be seen from the figure that substitution of Pr into  $\text{PbTiO}_3$  lattice, the value of dielectric constant at room temperature ( $\epsilon'_{\text{RT}}$ ) increases, while the maximum value of dielectric constant ( $\epsilon'_{\text{max}}$ ) and ' $T_C$ ' decreases. A small shift in the Curie temperature is also observed for almost all the composition at higher frequency which indicates some type of relaxational phenomenon occurring in these materials. Fig. 5 shows dielectric constant versus temperature at 1 kHz for various Pr substitutions in PT ceramics. One observe that when Pr substitution increases, the peak value of dielectric constant decreases except for  $x = 0.10$ . The increase in peak value of dielectric constant for  $x = 0.10$  is attributed to the change in the average grain size. As the average grain size of  $x = 0.06$  is less (507 nm) than for  $x = 0.10$  (531 nm), so, one would expect the increase in the dielectric constant value and hence increase in the peak value of dielectric constant. The maximum and minimum value of dielectric constant being for 0.04 and 0.08 mol% of Pr substituted composition, respectively. This decrease in  $\epsilon'_{\text{max}}$  implies that substitution of Pr reduces dipole moment of the lattice and lowers the peak value of dielectric constant. The transition temperature is also found to decrease with the increase in Pr substitution. This decrease in transition is attributed to decrease in crystal tetragonality caused by Pr substitution, which reduces the internal stress and which in turn reduces the transition temperature [13]. Decrease in transition temperature for  $x = 0.04, 0.06, 0.08$ , and  $0.10$  is shown in Fig. 6. The decrease in transition temperature has been observed in lanthanum and calcium modified PT ceramics [14–16]. Fig. 7 shows the variation of  $\epsilon'$  with frequency ( $10^3$ – $10^6$  Hz) from room temperature to  $500^\circ\text{C}$  for  $x = 0.04$ , which is normal dielectric/ferroelectric behaviour. It is observed that the value of dielectric constant of each specimen at higher frequency gets markedly dropped. This phenomenon can be explained in terms of interfacial polarization. This built up of charges at the grain–grain boundary interface is responsible for large polarization, therefore high dielectric constant at lower frequency [17]. Fig. 8 shows the variation of dielectric loss ( $\tan \delta$ ) with temperature for all the compositions at a fixed frequency. The loss in these materials is mainly due to structural inhomogeneity and domain wall movements, i.e., intergrain heat flow or grain rotation [18–20].

The region around the dielectric peak is broadened, which are diffuse phase transaction (DPT). This may be due to the disorder in the arrangement of rare earth (Pr) and other atoms, leading to a microscopic heterogeneity in the composition and

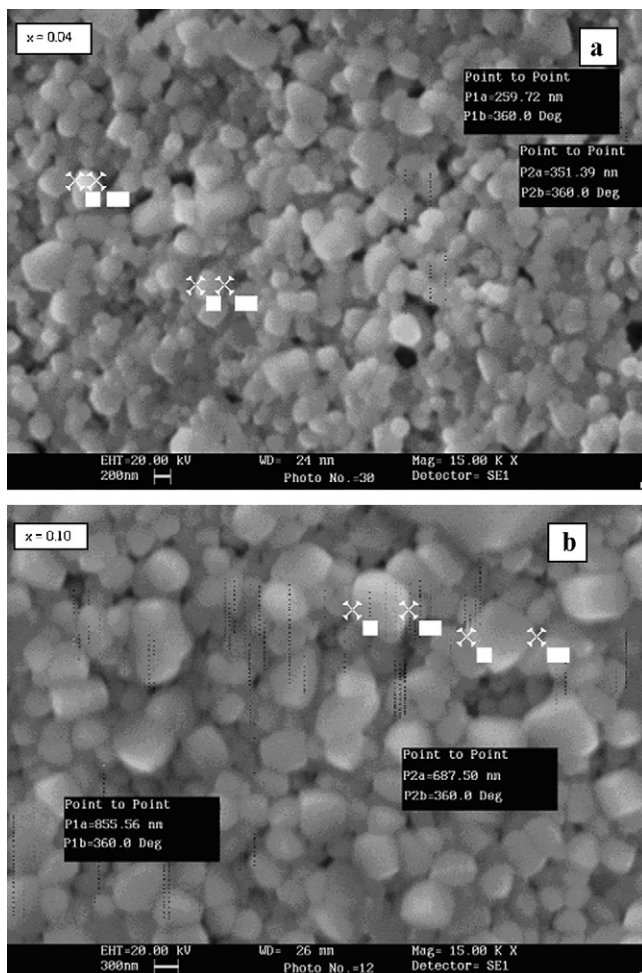


Fig. 3. Scanning electron microscopic (SEM) images of  $\text{Pb}_{1-x}\text{Pr}_x\text{Ti}_{1-2y}\text{Mo}_{3y}\text{Fe}_2\text{O}_7$  ceramics sintered at  $1100^\circ\text{C}$  for different compositions (a) 0.04, (b) 0.10.

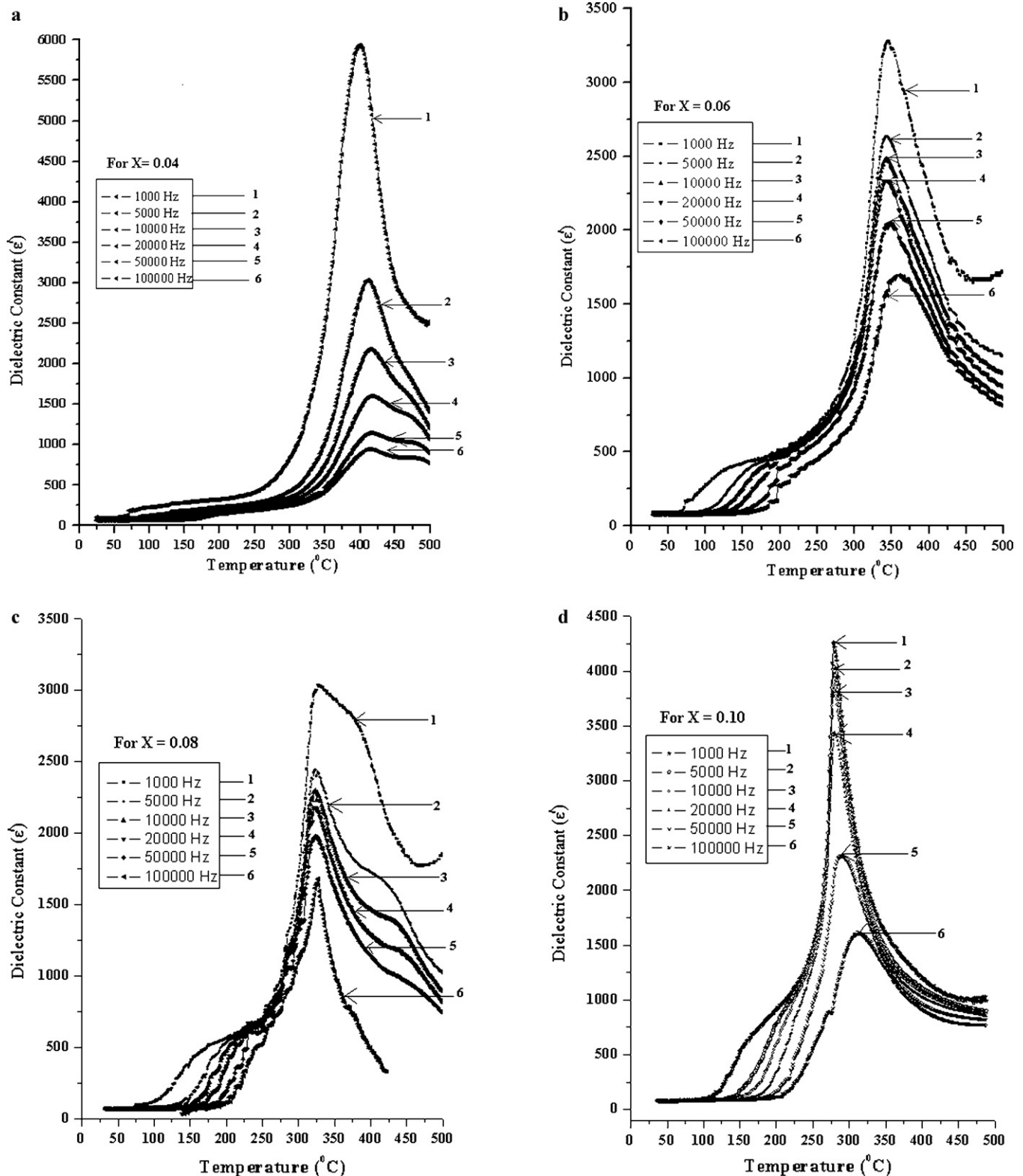


Fig. 4. Temperature dependence of dielectric constant at different frequency for Pr substituted lead titanate ceramics with compositions (a) 0.04, (b) 0.06, (c) 0.08 and (d) 0.10.

thus a distribution of different local curie points [21]. The structural disorder arises due to the presence of a number of voids and impurities of different size. The degree of diffusivity ( $\gamma$ ) can be calculated using the expression [22]:

$\ln(1/\epsilon' - 1/\epsilon'_{\max}) = \gamma \ln(T - T_C) + C$ ; where ' $\epsilon'_{\max}$ ' is the maximum value of dielectric constant at transition temperature, ' $\gamma$ ' is the degree of diffusiveness which lies in the range  $1 < \gamma \leq 2$ .  $\gamma = 1$  represent the ideal Curie Weiss behaviour,



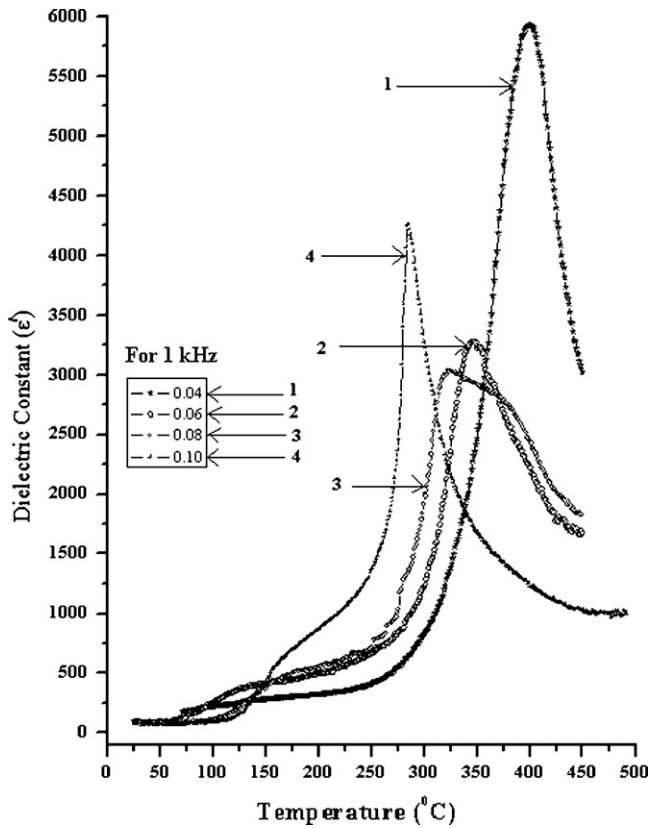


Fig. 5. Variation of the dielectric constant ( $\epsilon'$ ) with temperature at a frequency of 1 kHz for different praseodymium composition.

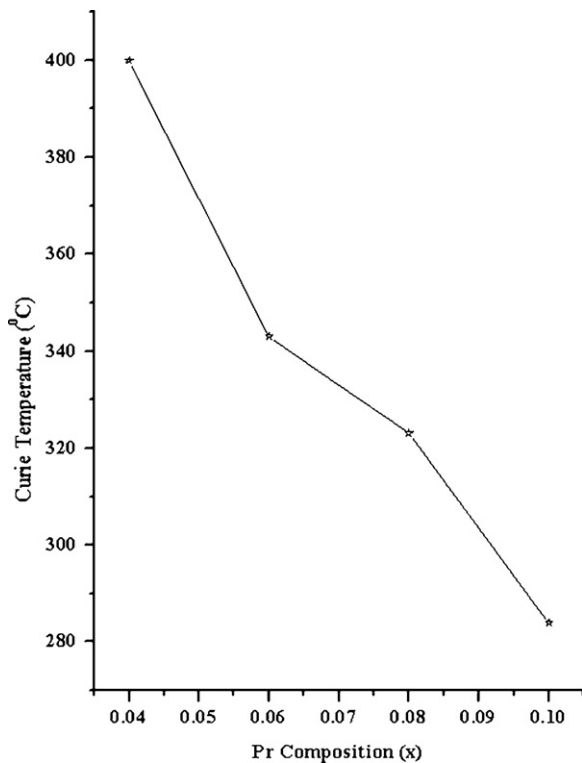


Fig. 6. Variation of Curie temperature ( $T_c$ ) with praseodymium composition ( $x$ ).

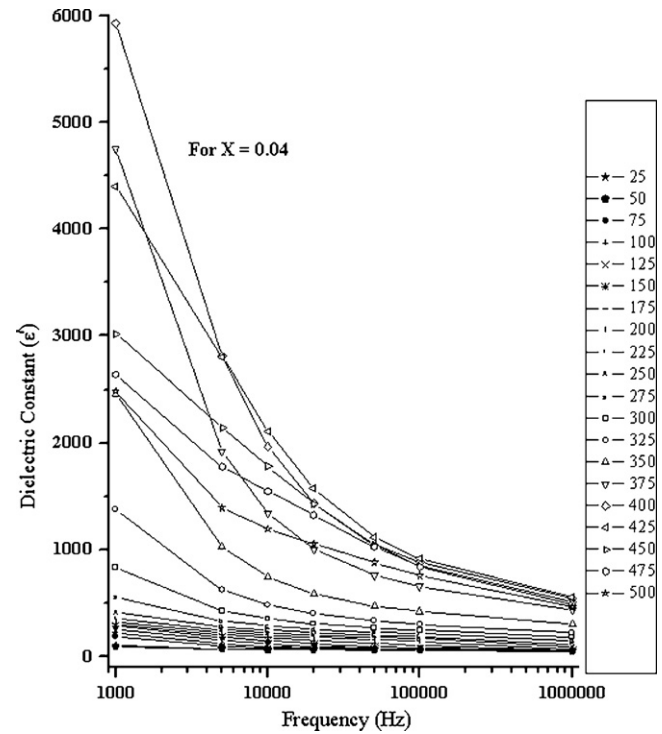


Fig. 7. Variation of dielectric constant with frequency at different temperature (25–500  $^{\circ}\text{C}$ ) for 0.04 of Pr substituted lead titanate ceramics.

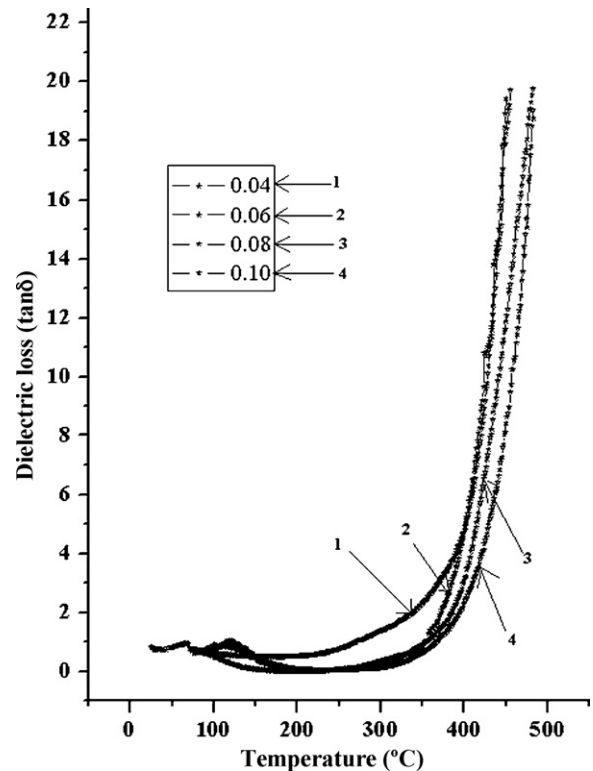


Fig. 8. Variation of dielectric loss ( $\tan \delta$ ) with temperature at a frequency of 1 kHz for 0.04, 0.06, 0.08 and 0.10 of Pr substituted lead titanate ceramics.

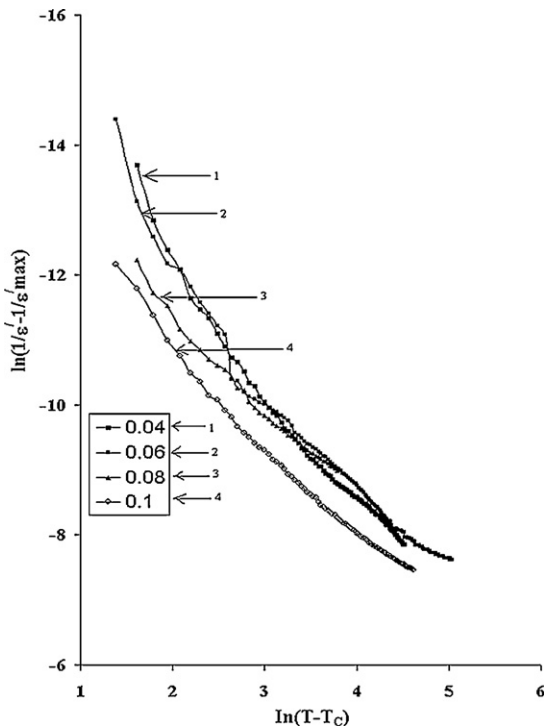


Fig. 9.  $\ln(1/\epsilon' - 1/\epsilon'_{\max})$  versus  $\ln(T - T_C)$  of praseodymium substituted lead titanate ceramics giving the values of diffused phase transition.

whereas ' $\gamma$ ' between 1 and 2 indicates diffuse phase transition [16]. The value of ' $\gamma$ ' is calculated from the slope of graph  $\ln(1/\epsilon' - 1/\epsilon'_{\max})$  versus  $\ln(T - T_C)$ . Fig. 9 shows the variation of  $\ln(1/\epsilon' - 1/\epsilon'_{\max})$  with  $\ln(T - T_C)$  at a particular frequency of 5 kHz for different composition, i.e.,  $x = 0.04, 0.06, 0.08, 0.10$  and it is found that the value of ' $\gamma$ ' comes out to 1.67, 1.46, 1.37, 1.32, respectively. This implies the diffuse phase transition, which may be due to the compositional fluctuations and structural disordering in the arrangement of cations in one or more crystallographic sites in the structure that finally results in a microscopic heterogeneity in the grown materials with local curie points [23,24].

### 3.2.2. AC conductivity and activation energy

The ac conductivity ( $\sigma_{ac}$ ) and activation energy ( $E_a$ ) of all the composition in the high temperature region was calculated from the measured dielectric data, using the formula [25]:  $\sigma = \epsilon' \epsilon_0 \omega \tan \delta = \sigma_0 \exp(-E_a/k_B T)$ ; where  $\epsilon_0$  is the free space permittivity, ' $\omega$ ' the angular frequency, ' $\tan \delta$ ' is the dielectric loss, ' $\sigma_0$ ' pre-exponential factor and ' $k_B$ ' the Boltzmann constant. The ac conductivity is plotted against the inverse of temperature at a frequency of 1 MHz and is shown in Fig. 10, which shows the change in slope almost at the same transitions temperature as is observed in case of dielectric studies. This change in the slope is due to the difference in activation energy in the paraelectric and ferroelectric phase, which is due to the grain boundary effect [26]. From the figure, one can clearly see that there is shift in the transition temperature from ferroelectric to paraelectric phase. This behaviour can be attributed to relaxational process associated with the domain reorientation, domain wall motion and the dipolar behaviour [23]. There are

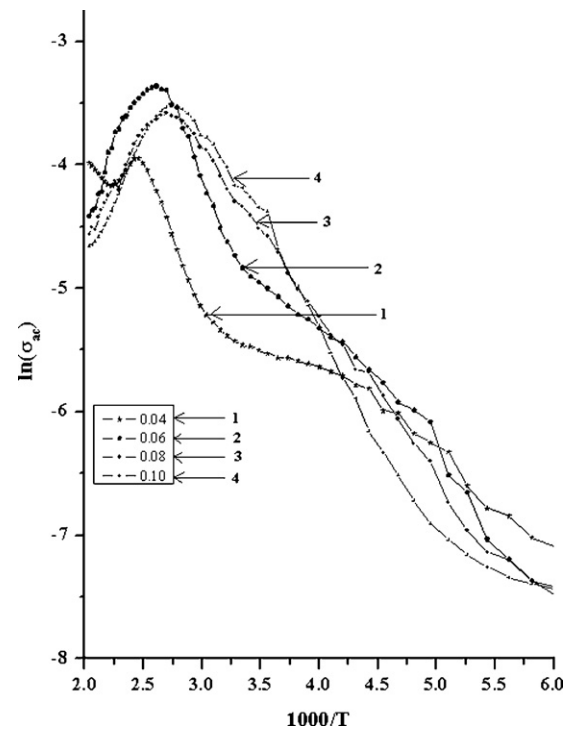


Fig. 10. Plot of  $\ln(\sigma_{ac})$  conductivity versus  $1000/T$ .

distinct region of conduction mechanisms in different temperature range (i)  $n$  and/or p-type hopping charge (corresponding to low temperature), (ii) small polarons and oxygen vacancy conduction (corresponding to intermediate temperature region) and (iii) intrinsic ionic conduction (at high temperature region) [27]. The nature of variation of ac conductivity ( $\sigma_{ac}$ ) for wide temperature range favours the

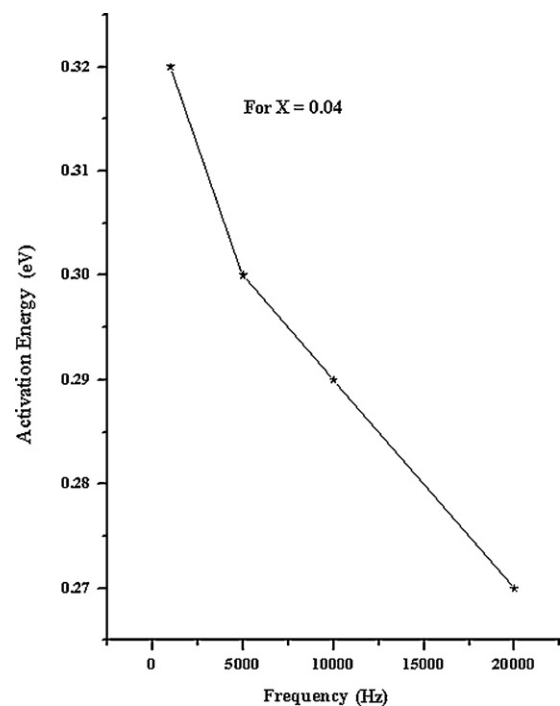


Fig. 11. Activation energy ( $E_a$ ) at different frequencies ( $\nu$ ) for 0.04 of praseodymium substituted lead titanate ceramics.

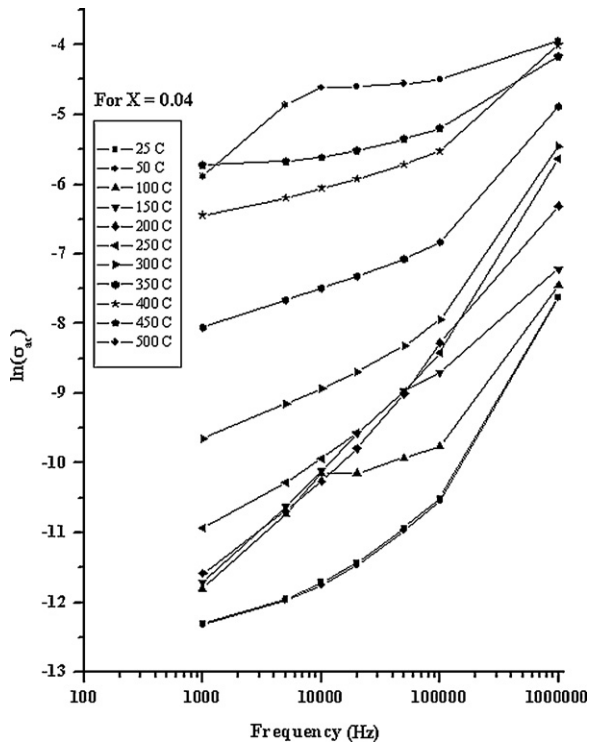


Fig. 12.  $\ln(\sigma_{ac})$  versus frequency ( $\nu$ ) at different temperatures (25–500 °C) for 0.04 Pr substituted lead titanate ceramics.

thermally activated transport properties obeying Arrhenius formula:

$\sigma = \sigma_0 \exp(-E_a/k_B T)$ . The activation energy ' $E_a$ ' is calculated at temperature in the ferroelectric region near the maximum where the loss tangents are relatively low. The activation energy is calculated from the slope of the graph of  $\ln(\sigma_{ac})$  versus  $T^{-1}$  for frequencies of, 1, 5, 10, 20 kHz. It can be seen from the graph (Fig. 11) of activation energy ( $E_a$ ) versus frequency ( $\nu$ ) for  $x = 0.04$  mol% of Pr substitution, that the activation energy decreases with the increase in frequency and magnitude of activation energy is greater than 0.2 eV. Same trend has been observed for all the composition, which suggests that conduction mechanism is due the hopping of charge carriers (i.e., n and p type) from one site to other [28]. Therefore, very small amount of energy is required to activate the charge carriers/electrons for electrical conduction. It has been shown by Ang et al. [29] and Moretti and Michel-Calendini [30] that the value of activation energy depends on ionization level of the oxygen vacancy. Usually, activation energy less than 1.0 eV is connected to singly ionized vacancies [29] and/or electronic mobility in space charge regions [31]. Thus, the conduction process within this temperature range may be due to the hopping of charge carriers and/or singly ionized oxygen vacancies of the ceramics. With a view to understand and authenticate the conduction mechanism, a.c conductivity ' $\ln(\sigma_{ac})$ ' is plotted as a frequency ' $\nu$ ' in the range of  $10^3$ – $10^6$  Hz for different temperature and is shown in Fig. 12. It is observed that a.c conductivity increases with increasing frequency at all temperature which is characteristics feature of material where hopping mechanism dominates. As frequency

increases, ac conductivity increases due to the strong mobility of charge carriers.

#### 4. Conclusion

Praseodymium modified lead titanate with composition  $\text{Pb}_{1-x}\text{Pr}_x\text{Ti}_{1-2y}\text{Mo}_y\text{Fe}_y\text{O}_3$ ; where  $x = 0.02, 0.04, 0.06, 0.08, 0.10$  and  $y = 0.02$  have been successfully synthesized by solid state reaction technique. XRD analysis of the sintered composition predicted that all the prepared samples are in pure perovskite phase with tetragonal structure. Grain size calculated from the scanning electron micrograph comes out to be in nano-meter thus suggesting formation of nano particles in Pr modified lead titanate ceramics. Increase in the amount of Pr decreases crystal tetragonality. The Curie temperature is found to decrease as function of composition ( $x$ ) which is due to decrease in stress in compositions containing higher Pr concentration. Phase transition is observed in all composition and nature of transition is found to be diffused with the degree of diffusivity ' $\gamma$ ' equal to 1.67, 1.46, 1.34 and 1.32 for  $x = 0.04, 0.06, 0.08$  and 0.10, respectively. The AC ( $\sigma_{ac}$ ) conductivity increases with the increase in frequency at all temperature suggests that hopping mechanism dominate.

#### Acknowledgement

The work was supported by DRDO, Government of India under its Grant in aid scheme and one of the authors Vishal Singh is working as senior research fellow (SRF) under the scheme. The support is thankfully acknowledged.

#### References

- [1] C.D. Chandler, C. Roger, M. Hampden-Smith, Chemical aspects of solution routes to perovskite-phase mixed-metal oxides from metal-organic precursors, *J. Chem. Rev.* 93 (1993) 1205–1241.
- [2] S. Liu, Z. Xiu, J. Liu, F. Xu, W. Yu, Combustion synthesis and photoluminescence of perovskite  $\text{PbTiO}_3$  nanopowders, *J. Alloys Compd.* 441 (2007) L7–L9.
- [3] M. Kellati, S. Sayouri, N. El Moudden, M. Elaatmani, A. Kaal, M. Taibi, Structural and dielectric properties of La-doped lead titanate ceramics, *Mater. Res. Bull.* 39 (2004) 867–872.
- [4] R. Pazik, D. Hreniak, W. Strek, A. Speghini, M. Bettinelli, Effects of dopants on the piezoelectric and dielectric properties of Sm-modified  $\text{PbTiO}_3$  ceramics, *Opt. Mater.* 28 (2006) 1284–1288.
- [5] M. Maeda, H. Ishida, K.K. Soe, I. Suzuki, Preparation and properties of  $\text{PbTiO}_3$  films by sol–gel processing, *J. Appl. Phys.* 32 (1993) 4136–4140.
- [6] J.B. Jaffe, W.R. Cook, H. Jaffe, *Piezoelectric Ceramics*, Academic Press, New York, 1971.
- [7] T. Takahashi, Lead titanate ceramics with large piezoelectric anisotropy and their application, *Ceram. Bull.* 69 (1990) 691–695.
- [8] H. Takenchi, S. Jyomura, E. Yamamoto, Y. Ito, Electro-mechanical properties of (Pb,Ln) (Ti,Mn) $\text{O}_3$  ceramics, *J. Acoust. Soc. Am.* 72 (1982) 1114–1120.
- [9] Y. Yamashita, K. Yokoyama, H. Honda, T. Takahashi, (Pb Ca)[(Co $_{1/2}$ W $_{1/2}$ )Ti] $\text{O}_3$  piezoelectric ceramics and their applications, *Jpn. J. Appl. Phys.* 20 (1981) 183–187.
- [10] R. Tickoo, R.P. Tondon, K.K. Bamzai, P.N. Kotru, Dielectric and piezoelectric characteristics of samarium modified lead titanate ceramics, *Mater. Sci. Eng. B* 103 (2003) 145–151.
- [11] J. A. Sudgen, US Patent No. 3068277.

- [12] S. Chu, C. Chem, Effects of dopants on the piezoelectric and dielectric properties of Sm-modified  $\text{PbTiO}_3$  ceramics, *Mater. Res. Bull.* 35 (2000) 2317–2324.
- [13] K. Okazaki, Mechanical behaviour of ferroelectric ceramics, *Ceram. Bull.* 63 (1984) 1150–1157.
- [14] R. Tickoo, R.P. Tandon, N.C. Mehra, P.N. Kotru, Dielectric and ferroelectric properties of lanthanum modified lead titanate ceramics, *Mater. Sci. Eng. B* 94 (2002) 1–7.
- [15] T. Yamamoto, H. Igarashi, K. Okazaki, Dielectric electromechanical, optical and mechanical properties of lanthanum modified lead titanate ceramics, *J. Am. Ceram. Soc.* 66 (1983) 363–366.
- [16] K. Prasad, Diffuse phase transition in perovskite ferroelectric, *Indian J. Eng. Mater. Sci.* 7 (2000) 446–450.
- [17] Z.H. Yao, H.L. Liu, Y. Liu, Z.H. Wu, Structure and dielectric behaviour of Nd-doped  $\text{BaTiO}_3$  perovskite, *Mater. Chem. Phys.* 109 (2008) 475–481.
- [18] K. Prasad, R. Sati, R.N.P. Chodhary, T.P. Sinha, Synthesis and electrical studies of modified  $\text{PbTiO}_3$  ceramics:  $(\text{Pb}_{1-x}\text{Ca}_x)(\text{Mn}_{0.05}\text{W}_{0.05}\text{Ti}_{0.90})\text{O}_3$ , *Bull. Mater. Sci.* 16 (1993) 679–684.
- [19] K. Prasad, R. Sati, R.N.P. Chodhary, K.L. Yadav,  $(\text{Pb,Ca})(\text{Mn}_{0.05}\text{W}_{0.05}\text{Ti}_{0.90})\text{O}_3$ : X-ray and dielectric studies, *J. Mater. Sci. Lett.* 12 (1993) 758–759.
- [20] C.M. Srivastava, C. Srinivasan, *Science and Engineering Materials*, Wiley Eastern Ltd, New Delhi, 1987.
- [21] M.E. Lines, A.M. Glass, *Principle and Application of Ferroelectric and Related Materials*, Oxford, 1997.
- [22] S.M. Pilgrim, Diffusenesses as a useful Parameter for Relaxor Ceramics, *J. Am. Ceram. Soc.* 73 (1990) 3122–3125.
- [23] L.E. Cross, Relaxor ferroelectrics, *Ferroelectrics* 76 (1987) 241–267.
- [24] C. Schmidt, Diffusive phase transitions, *Ferroelectrics* 78 (1988) 199–206.
- [25] V.M. Gurevich, Electric conductivity of ferroelectrics (Israel Program for scientific translation) (Jerusalem) 1971.
- [26] O.P. Thakur, C. Prakash, Dielectric properties of samarium substituted barium strontium titanate, *Phase transition* 76 (2003) 567–574.
- [27] O. Raymond, R. Font, N. Suarez-Almodovar, J. Portelles, Frequency-temperature response of ferroelectromagnetic  $\text{Pb}(\text{Fe}_{1/2}\text{Nb}_{1/2})\text{O}_3$  ceramics obtained by different precursors, *J. Appl. Phys.* 97 (2005) 084108.
- [28] I. Sirdeshmukh, K. Krishan Kumar, S. Bal Laksman, A. Ramakrishna, G. Sathish, Dielectric properties and electrical conduction in yttrium iron garnet (YIG), *Bull. Mater. Sci.* 21 (1998) 219–226.
- [29] C. Ang, Z. Yu, L.E. Cross, Oxygen- vacancy related low frequency dielectric relaxation and electrical conduction in Bi:  $\text{SrTiO}_3$ , *Phys. Rev. B* 62 (2000) 228–236.
- [30] P. Moretti, F.M. Michel-Calendini, Impurity energy levels and stability of Cr and Mn ions in Cubic  $\text{BaTiO}_3$ , *Phys. Rev. B* 36 (1987) 3522–3527.
- [31] N. Ortega, A. Kumar, R.S. Katiyar, J.F. Scott, Maxwell Wenger space charge effects on the  $\text{Pb}(\text{Zr Ti})\text{O}_3\text{--CoFe}_2\text{O}_4$  multilayers, *Appl. Phys. Lett.* 91 (2007), Article ID 102902.